Revista de Chimie
https://revistadechimie.ro
https://doi.org/10.37358/Rev.Chim.1949

Experimental Investigation of Two-Phase Flow Bubble Characteristics in Small Bubble Column using Electrical Capacitance Tomography

LOKMAN A. ABDULKAREEM*
University of Zakho, Department of Petroleum Engineering, P O Box 12, Northern Iraq

Abstract: *The present study has been carried out to investigate the characterization of two-phase flow bubbles that occurred in a column of an internal diameter 50 mm, where the liquid phase is represented in Silicone oil. The effectiveness of the tomography technique regarding the flow patterns analysis is studied as well as, high-speed videos were captured and used in the study. The void fractions of the time series were obtained at different flow rates were considered, and the results were analyzed also by using Probability Density Functions (PDF), film thickness, velocity structure, and Power Spectrum Density (PSD). To obtain the structure velocity, two tomography capacitance sensors were utilized so as to do cross-correlation, besides, the obtained videos were considered also to show the different bubble characteristics. A comparison was assessed between the previously available works of literature with the present study to evaluate the results. It was observed from the obtained tomography images that the flow was in the slug flow region explained by the presence of large bullet-shaped bubbles and the bubble characteristics obtained were comparable to that observed in other viscous liquids. Electrical Capacitance Tomography (ECT) was quite effective in investigating the flow.*

Keywords*: bubble column, electrical capacitance tomography, two-phase flow*

1. Introduction

The multiphase flow of different types of form is made up of the different combinations of the three different phases; gas, liquid, and solid. All the phases involved in the flow interact with each other making it more complex for the engineers to analyses the flow accurately. It is extremely important to have a crystal comprehension about this phenomenon because it is encountered in numerous industrial applications; the petroleum industry introduces a good example where it is encountered in both downstream and also in upstream processes. This paper emphasizes on gas-liquid flow in a bubble column and the effect of the different physical parameters on it. Experiments were also carried out in this study to evaluate the validation of the tomography technique in the flow analysis, in particular, the Electrical Capacitance Tomography (ECT) method used by Fossa [1] for determining the flow characteristics. Bubble columns are commonly existed in chemical industries for contacting both phases of liquid and gas, besides some cases even involve the third phase. It is fair to say that bubble columns are one of the most significant members among the gas-liquid contactors because of its many applications in chemical, petrochemical, pharmaceutical, and environmental industries [2]. Gas-liquid flow is a topic of great interest not only in the field of chemical engineering but also in other areas of engineering such as high-powered lasers, high-performance microelectronics, high heat-flux compact heat exchangers in spacecraft, medical devices, supercomputers, and others [3]. The homogeneous flow mainly consists of equally sized small bubbles distributed throughout the liquid even in the heterogeneous flow case there is a radial variation in bubble properties and they usually occur at higher gas velocities rather than at low velocities as in the case of homogeneous flow [4]. Apart from the above categorization of flow, some others have also been suggested for example Govier and Aziz [5], Lockett and Kirkpatrick [6], and Wallis [7] have characterized flow into three main regimes bubble flow, slug flow and churn flow regimes, (Figure 1).

**email:lokman.abdulkareem@uoz.edu.krd*

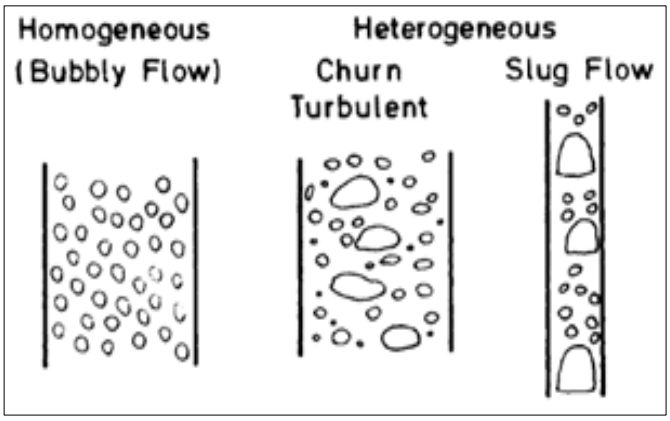

Figure 1. Diagrammatic representation of flow regimes in a bubble column Y.T Shah et al, [8]

Therefore, the main aim of the study is to characterize the flow of silicone oil in a bubble column of 50 mm and to study the effectiveness of the Electrical Capacitance Tomography method in determining the flow characteristics.

2. Materials and methods

Runs were conducted with silicone oil as a liquid phase, in addition to air which is used as the gas phase. All the runs were investigated completely in a column of internal diameter 50 mm. Silicone oil is a non-conductive liquid, then the Electrical Capacitance Tomography technique is utilized by Abdulkareem et al. [9] and used also for studying the flow patterns in this test. The below table shows the properties of the liquid used at room temperature.

Table 1. Fluid properties

Liquid	Density(g/cm 3)	Surface tension (N/m)	Viscosity (Pa.s)	Conductivity ($\frac{\mu S}{cm}$)	Dielectric constant
Silicone oil	2.53	0.736	0.35	0	11.8

2.1. Bubble column arrangement

A 50 mm acrylic resin pipe is used to assemble the column of bubbles in a vertically mounted position with the silicone oil fluid that carried out by Abdulkareem et al [10]. The used column was of 2 m height and the air phase was introduced into the column from the bottom through a porous glass sparger of 30 mm diameter. Two Electrical Capacitance Tomography sensors were used for flow measurement and the first sensor was kept at a height of 20 cm from the bottom and the spacing between the centers of the two sensors is fixed with a space of 15 cm. Schematic diagram of the rig and photo are shown in Figure 2.

2.2. Probability density function

The Probability Density Function (PDF) of the time-varying void fraction can be used to determine the type of flow [11]. In this method, the PDF was plotted against the void fraction. Theoretically, PDF can be defined as the derivative of a cumulative distribution function which in this case is the void fraction within a data range which is given by the below equation;

$$P(x) = \frac{d[V(x)]}{dx}. \quad (1)$$

where V(x) gives the probability of void fraction falling in between x and x+ x, where x is an infinitesimally small value $\int_{-\infty}^{\infty} P(x)dx = 1$, therefore the total area enclosed by the PDF should be equal

to one. Costigan and Whalley [12] divided flow into 6 different patterns based on different types of PDFs. The six different patterns explained by Costigan and Whalley are given in Figure 3.

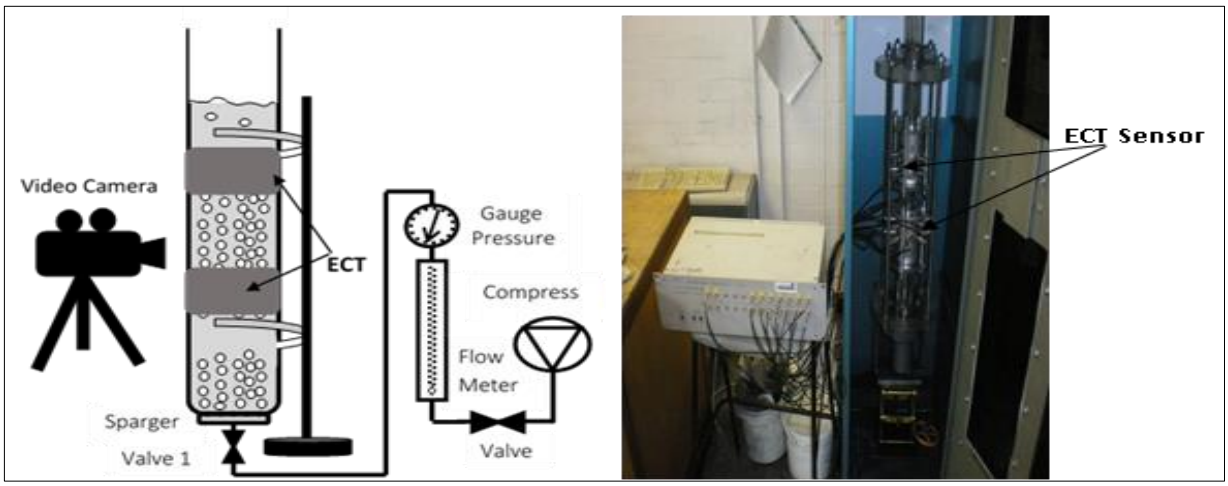

Figure 2. A-Schematic diagram of the Rig, B-photo of the Rig.

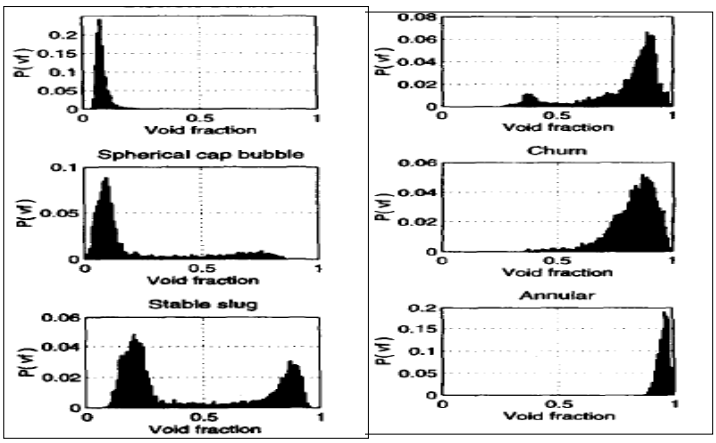

Figure 3. Different PDFs assigned for different flow types Costigan and Whalley [12]

3. Results and discussions

The results were obtained by the Electrical Capacitance Tomography (ECT) have been explained in the section below, and the data also were subjected to different analysis methods. Also, the results are compared with the results obtained from open literature.

3.1. The void fraction of time series

The Electrical Capacitance Tomography (ECT) provides time and cross-sectional resolved information about the spatial distribution of the phases. The time series of cross-sectional average void fraction allows detecting essential features of the flow. Void fraction time series were obtained under various conditions regarding superficial gas velocities. The time series here basically shows the variation of the void fraction with time. A buffer time of 60 s was fixed to take the measurements, thus a total of 12000 samples were obtained. The graphical plot in Figure 4 shows the variation of void fraction up to 60 s at low and high gas superficial velocities. The peaks in the figure show the big bubbles that are formed during the flow. These time-series graphs can be used for calculating the dominant frequency in a flow.

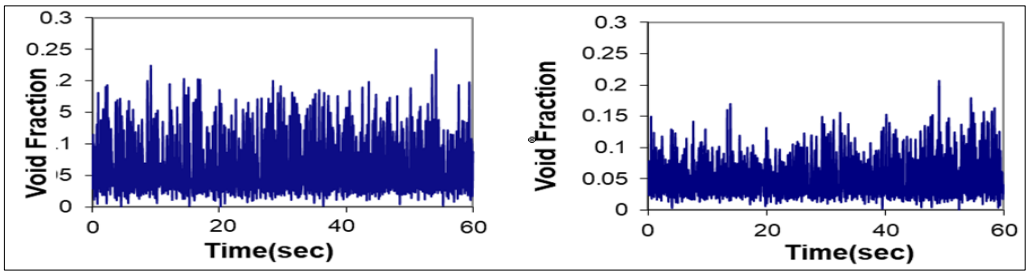

Figure 4. Time series of void fraction for low and high Gas Superficial Velocity

3.2. Mean void fraction

Mean void fractions were also calculated through each time series obtained at different gas flow rates and it was additionally plotted against the gas superficial velocities. Figure 5 shows the graphical plot of the variation of average void fraction obtained from both the sensors. As can be seen from the mentioned graph, the average void fraction from both sensors is found to undergo little change to a velocity of about 0.008 m/s, and after this point; both sensors show the average void fraction increasing monotonically with gas superficial velocity. It can also be seen that the average void fraction shown by sensor 2 was lesser than the corresponding values showed by sensor 1.

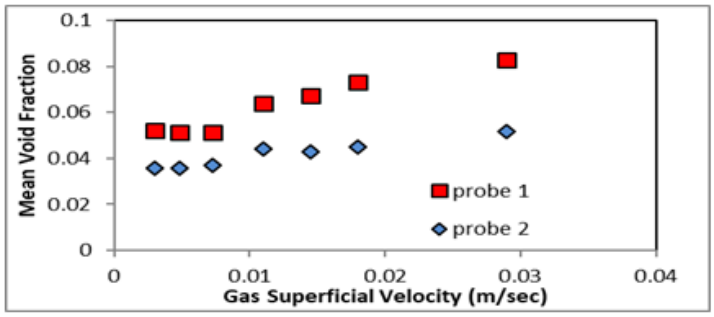

Figure 5. A plot of mean void fraction obtained from the two probes against Gas Superficial velocity

In Figure 6, the present work has been tested against the correlations proposed by Krishna et al [13], and the runs at low velocities were found to agree with the correlation but there was a significant deviation for a high superficial velocity of the gas. Another main difference in the present results obtained from that of the correlation is the absence of a change in slope signifying the transition from homogeneous flow regime to heterogeneous regime. This implies the absence of any transition occurring in the present studies.

The behavior of silicone oil was compared with the results obtained by Khaji et al. [14] with glycerol, ionic liquid, and water in a bubble column in Figure 7.

The comparison was made over the range of gas superficial velocities over which the present set of experiments were carried out, and silicone oil was found to follow a comparable trend to the other viscous liquids that were used by them, the slight change could be explained by the difference in electrode configurations which brings about a time delay. The average void fraction values were found to be around the same range as the other two viscous liquids with not much difference seen between their magnitudes at any gas superficial velocity, but the void fraction was found to be becoming lesser compared to ionic liquid and glycerol at higher gas superficial velocities. This can be explained because of the larger viscosity of silicone oil compared to glucose and ionic liquid, because of the absence of a small bubble population in more viscous liquids Urseanu et al. [15].

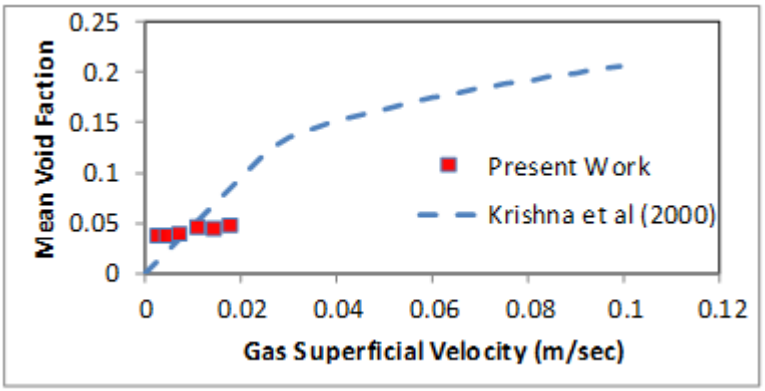

Figure 6. Comparison of present results with the correlation of Krishna et al. [11]

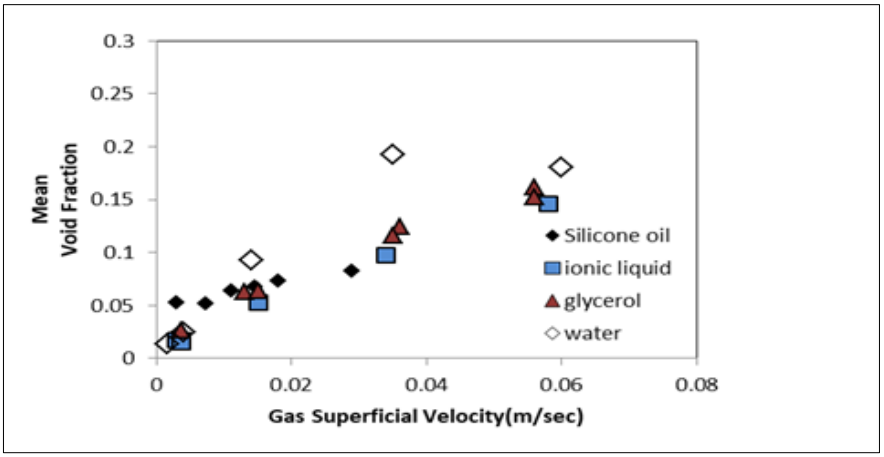

Figure 7. Comparison of the results obtained with Khaji et al. [14]

The present data were also compared with the data obtained by Urseanu et al. [15] in a larger column in Figure 8 and it was found that silicone was following the same trend as Tellus solution and an aqueous sugar solution with dynamic viscosities 0.07 and 0.17 respectively, but the average void fraction obtained using silicone oil was found to be greater than that obtained in larger columns by Urseanu et al. [15].

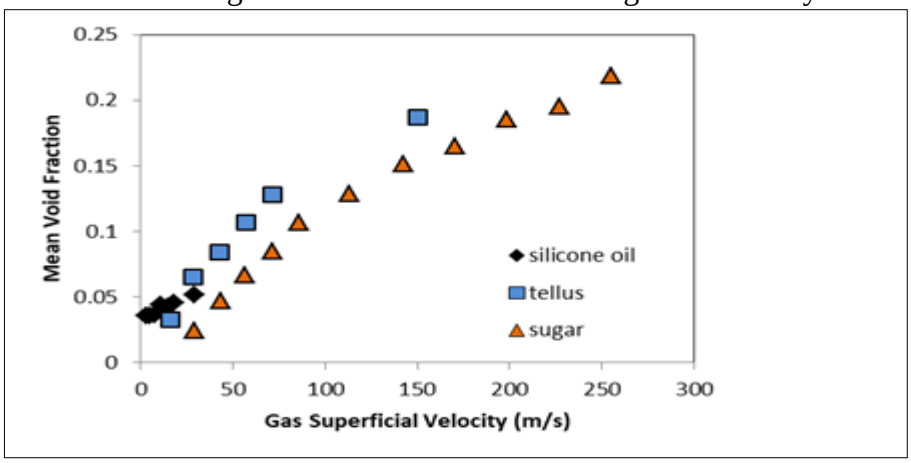

Figure 8. Comparison of present results with the results obtained in a 150mm bubble column Urseanu et al. [15]

The average void fraction was then plotted against the mean void fraction calculated over the entire time series. The plot has been shown in Figure 9. From the figure, it can be seen clearly that fluctuations from the mean value with an increase in flow rate. This shows that initially at low flow rate the flow is

bubbly, where the void fraction fluctuation is not big whereas at higher flow rates the flow is completely slugged thereby causing big fluctuations from the mean value.

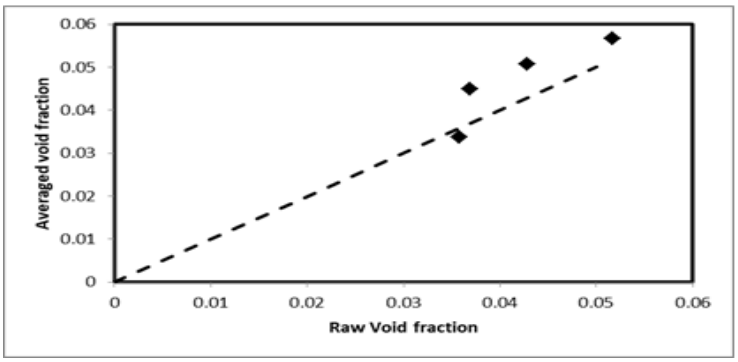

Figure 9. Comparison of average void fraction against mean void fraction for silicone oil

This, when compared with the video, explains that the flow is bubbly at lower flow rates with small spherical capped bubbles whereas with an increase in flow rate the flow pattern becomes slug with the formation of large bullet-shaped Taylor bubbles.

3.3.Probability density function (PDF)

The PDF of time-varying void fraction data is a very useful method for determining the type of flow. The PDF obtained for gas velocities of 0.005m/s, 0.02m/s, and 0.04 m/s from the electrical capacitance tomography is given in the Figure 10. The frequency was calculated after distributing the void fraction among the bins. The probability was then calculated by dividing each of the frequency values with the total number of data points. A logarithmic scale was applied to the y-axis to clarify the changes occurring as the peaks at lower void fraction are found to be quite small. For all the flows except when the superficial gas velocity is kept fixed at 0.005 m/s presence of the Taylor bubble is confirmed by the presence of the second peak in both the plots. Also, the distribution area for each PDF was found to increase with gas superficial velocity implying the increase in average void fraction with an increase in the gas superficial velocity.

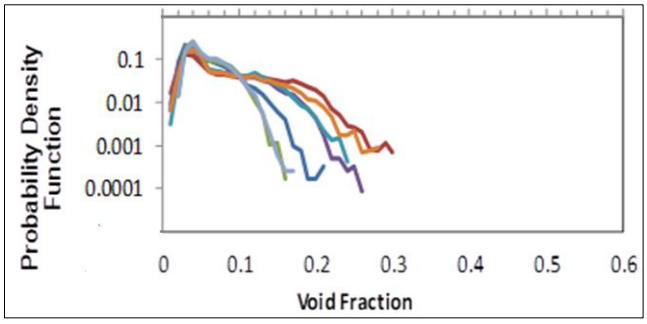

Figure 10. PDF of time-varying Void fraction obtained from ECT

In Figure 11, the PDF is obtained at different flow rates and compared with the results obtained with Khaji et al. [14]. It is clear from the above plot in Figure 11 that the behavior of the present work is similar to that of other viscous liquids like glycerol and ionic liquid. However, the distribution area occupied by the present work is found to be considerably less than that occupied by both glycerol and Ionic liquid, which means the average void fraction obtained with silicone oil is less than that obtained with Ionic liquid and Glycerol. This, however, shows that average void fraction occupied by silicone oil at a gas superficial velocity of 0.03 m/s was less than average void fraction obtained by Khaji et al. [14] with

glycerol and Ionic liquid. The presence of Taylor bubbles as seen during the flow is confirmed by the presence of the second peak implying that flow was slug flow.

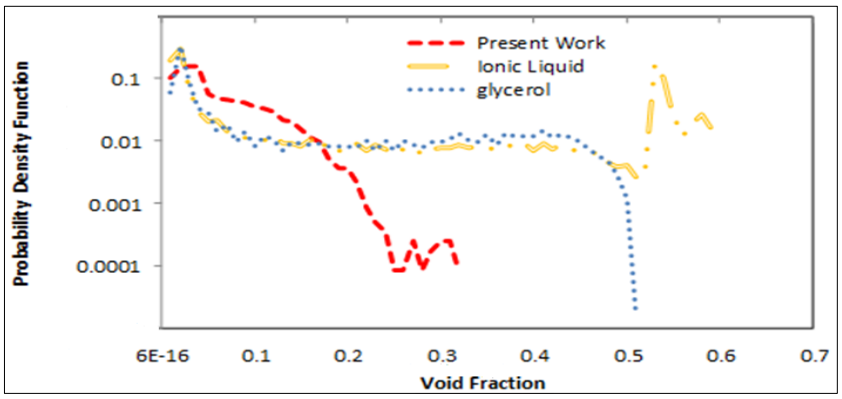

Figure 11. Comparison of PDFs of the present experiment with the PDFs obtained by Khaji et al. [14]

3.4.Structure velocity

Structure velocity is obtained by the cross-correlation of the void fraction data obtained from the two different capacitance sensors probe 1 and probe 2. Cross-correlation measures the similarity between the signals between the two probes; this is represented by the correlation coefficient which is plotted against the time lag. The structure velocity is then calculated from this time lag by dividing the distance between the centers of planes by the time lag.

The structure velocity thus calculated is then plotted against the gas superficial velocity. In the present case, the mixture velocity is equal to the gas superficial velocity because the liquid is kept still. The plot obtained is shown in Figure 12 and it can be seen from the graph that it varies linearly with the gas superficial velocity. Structure velocity has been found to increase almost uniformly with the mixture velocity. The plot was found to have a positive slope throughout the range of velocities over which the runs were done, indicating the absence of transition of flow pattern. However, the results here were found not to agree with Nicklin et al. [16] correlation with the deviation from it increases with the increase in gas velocity. it shows linear behavior expected in slug flow.

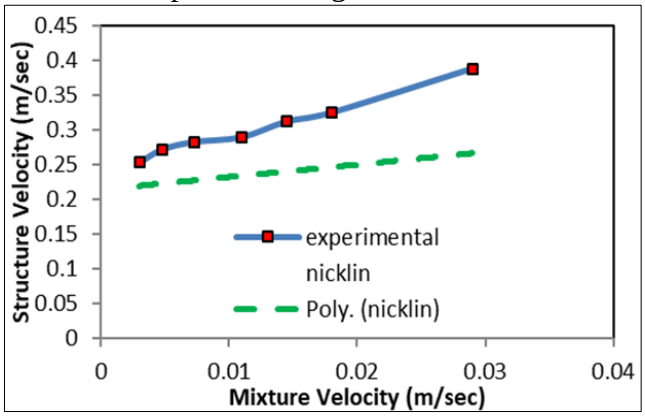

Figure 12. A plot of Structure velocity against Mixture velocity

The bubble velocities obtained in the present study were compared with the bubble velocities obtained by Kaji et al [14] with ionic liquid in Figure 13. It was seen that their magnitudes are very similar. This suggests that bubble behavior for both liquids can be considered to be similar in a column of the same diameter.

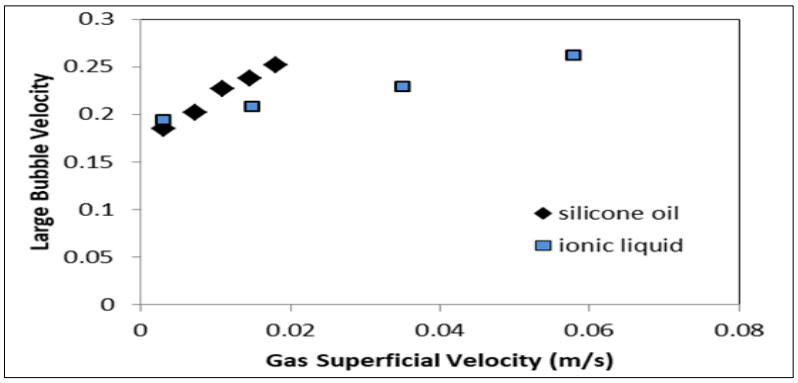

Figure 13. Comparison of bubble velocity of silicone oil with bubble velocity of the ionic liquid

The time delay at each flow rate was calculated by dividing the length of the electrodes with the structural velocity obtained at that particular flow rate. It is significant in cases where comparisons have to be made between flow characteristics obtained using two tomography techniques with different configurations for the sensor electrodes. Figure 14 shows the variation of an expected time delay with gas superficial velocity and it can be seen that the time delay linearly falls with the gas velocity.

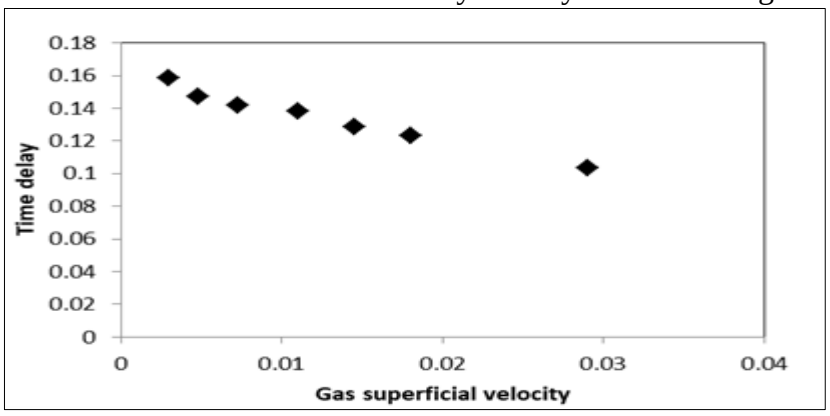

Figure 14. Variation of a time delay with Gas superficial velocity

3.5.Frequency and Power Spectral Density (PSD)

The dominant frequency at different flow rates has been obtained by two different methods for analysis, one from the peak of the PSDs obtained at each flow rate and the second by counting the number of peaks manually in the time series. The first set of values has been shown by the filled markers whereas the next set has been represented by the unfilled markers. The dominant frequency obtained by both methods has been plotted against the gas superficial velocity in Figure 15.

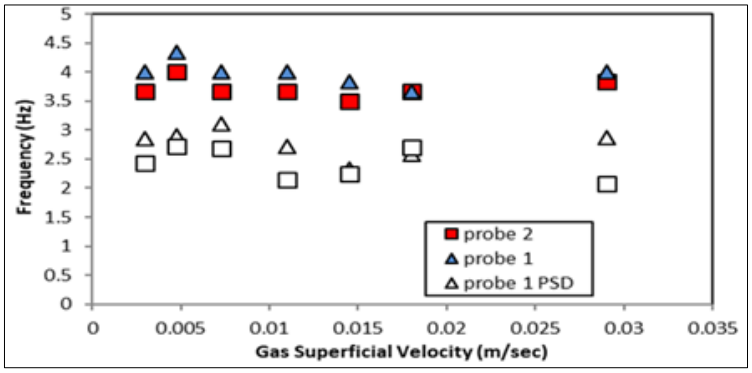

Figure 15. The plot of Dominant Frequency against Gas Superficial velocity

Clearly, the values of frequency remained relatively constant with slight variation. However, the dominant frequencies obtained from PSD were found to undergo fluctuations and a significant difference was found in the values of frequencies obtained from the two different methods with up to 85% variation at 0.03 m/sec. The PSD was also plotted against frequency, and the peak at all the flow rates was found to lie between 1.5 and 2.5 Hz. The plot is shown in Figure 16.

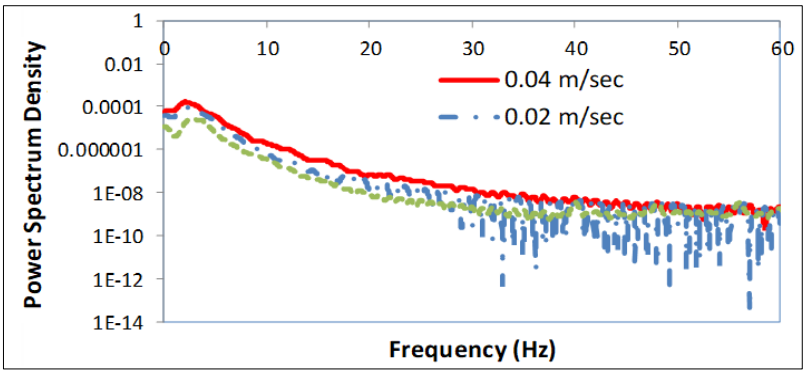

Figure 16. The plot of PSD against Frequency

It was found that the frequency was not found to undergo much change and this pattern was compared to the pattern obtained by Khaji et al. [14] with glycerol and Ionic liquid. The comparison is shown in Figure 17. As clearly seen from the plot trend obtained in the present study was found to be significantly different from that obtained by them, here the frequency was found to fluctuate with superficial gas velocity unlike what they have obtained with glycerol and ionic liquid where the frequency was found to fall with an increase in the gas superficial velocity. This fluctuation in frequency value is thought to be mainly caused due to disturbance caused by noise. However, the peak values of frequencies obtained for the present experiments were found to be in the same range as those obtained by them over the same range of gas flow rates showing that the slug structures were similar between viscous liquids.

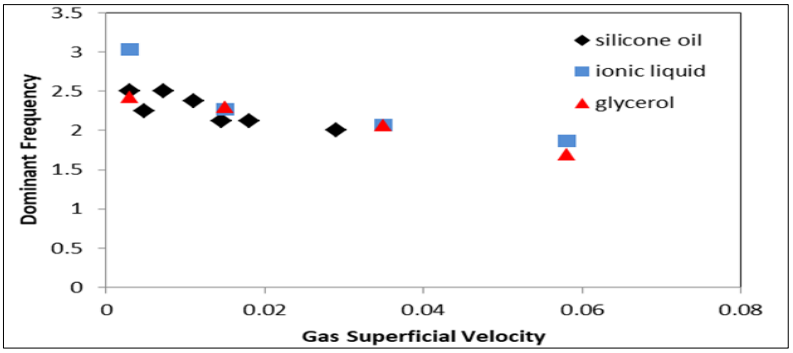

Figure 17. Comparison of dominant frequencies (obtained from PSDs) of the present experiment with those obtained by Khaji et al. [14]

Figure 18 shows that the difference between frequencies calculated by both counting method and from PSD lies mostly within +10%, however, the maximum deviation is found to be even more than -20%. The percentage variation obtained from the two probes was found to be not very different indicating that the slug structure was not changing much.

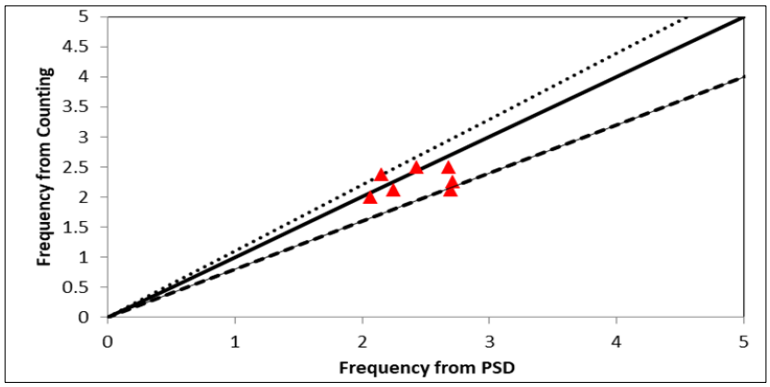

Figure 18. The difference in frequencies obtained by counting method and from PSD

3.6.Film thickness

Film thickness for a flow is calculated by the following equation;

$$Film\ thickness = \left(\frac{D}{2}\right) * \left(1 - \sqrt{\varepsilon_g}\right). \quad (2)$$

where D is the diameter of the tube and ε_g is the void fraction. The average film thickness is estimated for the various gas velocities that have plotted in Figure 19, which shows a steeply decrease in the film thickness with the increment values of the gas flow rate. Here the average film thickness was calculated from the average void fraction calculated for each flow rate, and it can be clearly seen from the plot that film thickness falls with an increase in the gas superficial velocity. This denotes the increase that occurred in the size of the bubbles with an increase in gas flow rate. It can also see that film thickness falls with height as indicated by the results given from the two planes. This shows the increase in bubble size with height.

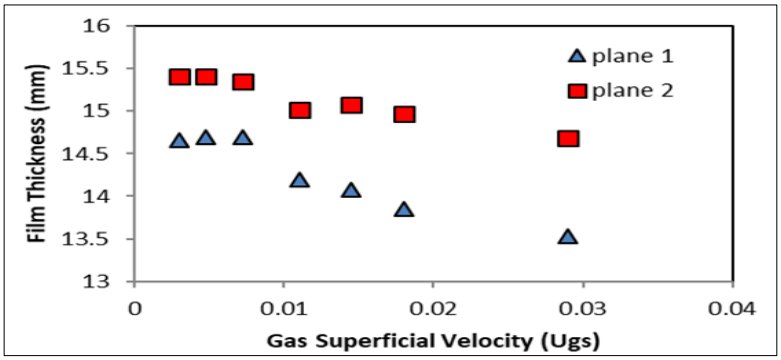

Figure 19. The plot of Average film thickness against gas superficial velocity

3.7.Video Analysis

As mentioned previously, the captured videos were collected using the high-speed camera then they were converted into a form of frames. These videos were also used for calculating the velocity of the large bubbles.

It can be clearly seen from Figure 20 that spherical cap bubbles were produced at a low flow rate, Their shape was found to change gradually from large spherical capped bubbles to bullet-shaped Taylor bubbles which characterize slug flow. The size of the bubbles formed was found to increase with the increase in gas flow rate. It was found from the videos that two main types of bubbles were formed the spherical cap or the bullet-shaped bubbles for higher flow rates and very small spherical bubbles. The very small spherical bubbles didn't coalesce with the large bubbles but were forced aside by the

approaching larger bubble and the smaller bubbles were then found to follow the larger bubbles. The smaller bubbles formed appeared to be suspended in the liquid and there was no coalescence between them as well, however, the larger bubbles were found to coalesce together and increase in size

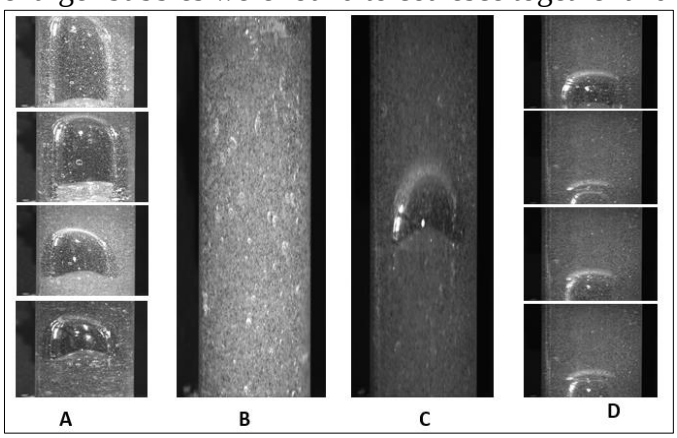

Figure 20. A- Images were taken from High-speed video at different gas flow rates of (0.003, 0.00727, 0.0145, 0.018), B- Cluster of bubbles, C- Small Spherical Cup Bubble D- Coalescence of bubbles Small spherical capped bubble and Cluster of bubbles

In Figure 21 the characteristics of the flow in the present study are compared with those of Kaji et al., [14]. They had done their experiments in a 38mm diameter bubble column with Ionic liquid, Glycerol+15% water and Glycerol+15% water+1.3% salt. Taylor bubbles were observed at much smaller gas velocities as compared to ionic liquid and glycerol solutions. However, in the case of the larger column in the present study no large bubbles were observed, this can be explained by the breakup of larger bubbles at higher gas flow rates due to liquid turbulence and smaller bubbles Azzopardi, [17].

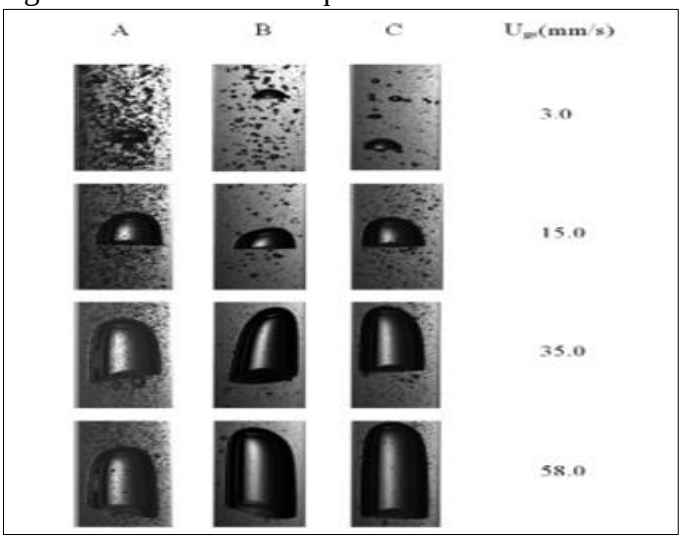

Figure 21. High speed video of bubbles produced in a 38 mm bubble column; A=ionic liquid, B= glycerol+15% water, C= glycerol+15% water+1.3% salt

3.8.Large bubble velocity

Large bubble velocity was calculated from the videos using Phantom 675 software. The calculation was done by the 2-point method. In this method, we have to select the large bubble first and then click on the leading edge of the bubble in two different frames. The software calculates the velocity of the bubble based on the time lag and the distance traveled by it. The large bubble velocity that was thus measured was then plotted against the gas superficial velocity in Figure 22. The resulting plot was then compared

against White and Beardsmore [18] correlation where the velocity was given by $0.33\sqrt{gD}$ where g is the acceleration due to gravity and D is the diameter of the column, and it was seen that the plot agrees reasonably with the plot but it was found to deviate more and more from the correlation with an increase in gas flow rate.

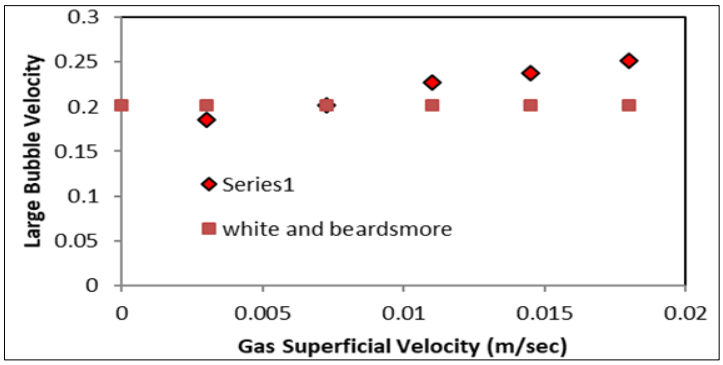

Figure 22. The plot of Large Bubble velocity against Gas Superficial velocity

Figure 23 shows the comparison of large bubble velocities of silicone oil and ionic liquid. It can be seen that with the increase in gas superficial velocity the difference between the two widens. Thus, at higher gas flow rates, large bubbles travel faster in silicone oil as compared to ionic liquid thereby time delay expected for silicone oil would be smaller than that expected of the ionic liquid.

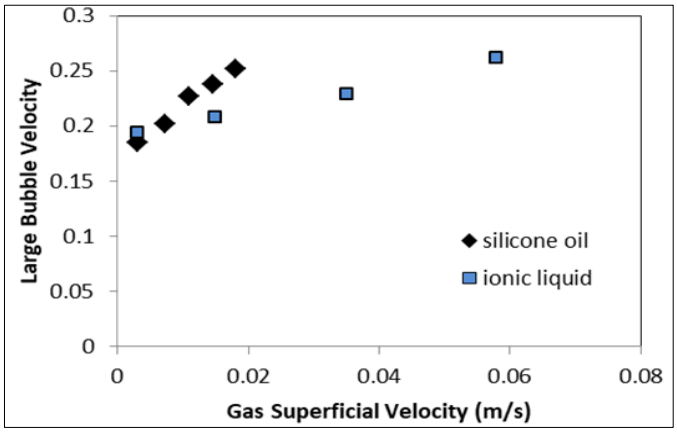

Figure 23. Comparison of large bubble velocity in silicone oil and ionic liquid

4. Conclusions

The following conclusions were made from the results obtained;

Taylor bubbles were observed from the results at higher flow rates whereas spherically shaped bubbles were observed at the lower flow rates thereby characterizing the type of flow as slug flow at higher flow rates. The larger bubbles produced were seen to coalesce together whereas the smaller spherical bubbles were found to move in clusters and retain individual characteristics.

The average void fraction was found to vary monotonically with the gas superficial velocity and it was not found to deviate much at low flow rates indicating less variation in a void fraction at lower flow rates indicating the presence of a bubbly flow regime at low flow rates. The frequency was not found to have any particular pattern of change with gas superficial velocity. Structure velocity was calculated using cross-correlation and it was found to change linearly with the gas superficial velocity as expected in slug flow. PDF's obtained at the different flow rates also confirm Slug flow.

The average film thickness was calculated at the different flow rates and it was found to decrease with an increase in the gas superficial velocity. ECT system has been fairly effective in analyzing the flow pattern, except for frequency measurements where fluctuations in measurements were seen.

References

1. FOSSA, M., Design and Performance of a conductance probe for measuring the liquid fraction in two-phase gas-liquid flows, *Flow measurement and Instrumentation*, 9, 1998, 103-109.
2. RIBEIRO, C.P., MEWES, D., The influence of electrolytes on gas hold-up and regime transition in bubble columns, *Chemical Engineering Science*, 62, 2007, 4501-4509.
3. SATITCHAICHAROEN, P., WONGWISES, S., Two-phase flow pattern maps for vertical upward gas-liquid flow in mini-gap channels, *International Journal of Multiphase Flow*, 30, 2004, 225-236.
4. RUZICKA, M.C., ZAHRADN, J., DRAHOS, J., THOMAS, N.H., Homogeneous–heterogeneous regime transition in bubble columns, *Chemical engineering science*, 56, 2001, 4609-4626.
5. GOVIER, G. W., & AZIZ, K., The flow of complex mixtures in pipes, *Journal of Fluid Mechanics By Nostrand Reinhold*, **65** (4), 1972, 825-827.
6. LOCKETT, M. J., & KIRKPATRICK, R. D., Ideal bubbly flow and actual flow in bubble columns, *Transactions of the Institution of Chemical Engineers*, 53, 1975, 267-273.
7. WALLIS, G.B., One-Dimensional Two-Phase Flow, McGraw-Hill Book Company, 1969.
8.Shah. Y.T, Kelkar. B.G and Godbole. S.P, Design parameters estimations for bubble column reactors, *AICHE Journal*, **28** (3), 2016, 353-379.
9. ABDULKAREEM, L.A., AZZOPARDI, B.J, HUNT, S., MARCO, A., DA SILVA, J., Interrogation of gas/oil flow in a vertical using two tomographic techniques, *proceedings of the asme 28th international conference on ocean, offshore and arctic engineering omae 2009, may 31-june 5, Honolulu, Hawaii*, 2009.
10. ABDULKAREEM., L.A., HAMID, S., Interrogation of bubble characteristics in two phase gas-liquid bubble column, *16th International Symposium on Flow Visualization June 24-28, Okinawa,Japan*, 2014.
11. ABDULKAREEM, L.A., ESCRIG, E., REINECKE, S., BUDDHIKA, N., AZZOPARDI B.J., Tomographic Interrogation of Gas-Liquid Flows in Inclined Risers, *International Multiphase Flow Conference, Florence, Italy*, 2016.
12. Costigan, G. and Whalley, P. B., "Slug Flow Regime Identification from Dynamic Void Fraction Measurements in Vertical Air-Water Flows", *International Journal of Multiphase Flow*, **23**, 1997, 263-282.
13. KRISHNA, R., URSEANU, M.I., DREHER. A.J., Gas hold-up in bubble columns: influence of alcohol addition versus operation at elevated pressures, *Chemical Engineering and Processing*, **39**, 2000, 371-378.
14. KHAJI.R, Z.D., LICENSE, P., AZZOPARDI, B.J., Studies of Ionic liquid and a gas in a small-diameter bubble column, *Ind. Eng. Chem*, **48**, 2009, 7938-7944.
15. Urseanu. M.I, Guit.R.PM, Stankiewicz.A, van Kranenburg.G, Lommen.J.H.G.M., Influence of operating pressure on the gas hold-up in bubble columns for high viscous media, *Chemical Engineering Science*, **58**, 2003, 697–704.
16. NICKLIN D, J., WILKES, J.O., DAVISON, J.F., Two Phase Flow in Vertical, 1962.
17. Azzopardi.B.J (2006), Gas Liquid Flows, *Wallingford, Begel House*, 2006.
18. WHITE, E.T., & BEARDMORE, R.H., The velocity of rise of single cylindrical air bubbles through liquids contained in vertical tubes. *Chem. Eng. Sci.*, **17**, 1962, 351-361.

Manuscript received: 12.11.2019